PHYSICAL REVIEW C, VOLUME 60, 014902

Multiple scattering effects in proton-nucleus collisions and the behavior of the total and partial inelasticities

M. Batista and R. J. M. Covolan
Instituto de Física Gleb Wataghin, Universidade Estadual de Campinas, Unicamp, 13083-970 Campinas, SP, Brazil
(Received 13 January 1999; published 16 June 1999)

A modified version of a multiple scattering model is applied to describe nuclear inclusive reactions of the type $pA \to pX$ and investigate the behavior of the inelasticity in nuclear processes. The modifications are such that some recent developments in the Pomeron physics are incorporated into the new theoretical scheme. The particular attention paid to the diffractive region of the spectrum results in a very good description of the diffractive cross section in terms of the atomic mass. Another important outcome resulting from this analysis is the average total inelasticity whose atomic mass and energy dependences are shown to be in agreement with the available data. Moreover, the behavior of partial inelasticities in intranuclear collisions is also discussed. [S0556-2813(99)00907-3]

PACS number(s): 13.85.Ni, 11.55.Jy, 13.85.Tp, 24.10.Ht

I. INTRODUCTION

Phenomenological models able to describe proton-nucleus interactions have been discussed extensively in the literature, and continue being an object of attention due not only to their intrinsic interest, but also to their importance to the analysis of high energy processes in both heavy ion collisions and cosmic-ray physics. In the latter case, for instance, they are crucial to estimate (via cascade generators) the energy of the primary particles interacting at the top of the atmosphere. Of particular interest in heavy ion collisions is, for example, the possibility for quark-gluon plasm formation which depends directly on the amount of energy deposited in the central rapidity region. A key quantity in both cases is the so-called inelasticity parameter whose behavior is the object of analysis in the present paper.

In a recent article [1], we have proposed a model (hereafter called BC model, for brevity) inspired in the Regge-Mueller formalism which, through an appropriate combination of contributions for the central and fragmentation regions, was able to give a good description of the inclusive spectrum of the proton in pp collisions in the whole phase space.

In the present paper, we extend our analysis to nuclear inclusive reactions of the type $pA \to pX$ by using a multiple scattering model which was initially proposed by Hwa [2], with further developments introduced by Hüfner and Klar (HK) [3] and Frichter, Gaisser, and Stanev (FGS) [4]. In all of these approaches, Feynman scaling is assumed. The theoretical framework employed here (which could be called FGS/BC approach) consists basically in introducing the BC model into the FGS formalism to compute the multiple scattering effects. In doing so, some additional assumptions[1] besides those of the original FGS model are required, but we believe they are reasonable and completely justified by the good description obtained for the experimental data.

In the present analysis, special attention is dedicated to the diffractive component of the cross section. Instead of just introducing it via the $(1/M^2)$-dependence (as is usually done in such an analysis), we perform specific calculation for this region of the spectrum and compare the results to the available data.

In short, we show that the combination of the BC and FGS models produces a very good overall description of the $pA \to pX$ data in all regions of the spectrum. This is done with only one free parameter that regulates the elasticity of the collisions in the nuclear medium. Since the BC model provides the energy dependence which is characteristic of the Regge pole formalism, no additional adjustments are necessary to obtain such a behavior for the nuclear cross sections and for the other quantities that are studied.

The paper is organized as follows. In Sec. II, we give a summarized description of the BC model and present some of its characteristic results. In Sec. III, we show how the BC model is applied to the FGS approach in order to obtain a theoretical framework used to describe $pA \to pX$ reactions. Descriptions of the experimental data and an analysis about the inelasticity behavior are shown in Sec. IV. Finally, our main results are summarized in Sec. V.

II. THE BC MODEL

The description of the leading proton spectrum presented in Ref. [1] was established according to the reaction mechanisms dominant at the central and fragmentation regions whose cross sections can be derived within the Regge-Mueller formalism [5]. In such a description, the central region is dominated by double Reggeon[2] exchanges and the respective invariant cross section is given by

[1]For instance, the BC model, which is based on the Regge-Mueller formalism, incorporates Feynman scaling breaking in a natural way.

[2]The designation Reggeon here stands for the usual secondary Reggeons and for the Pomeron as well.

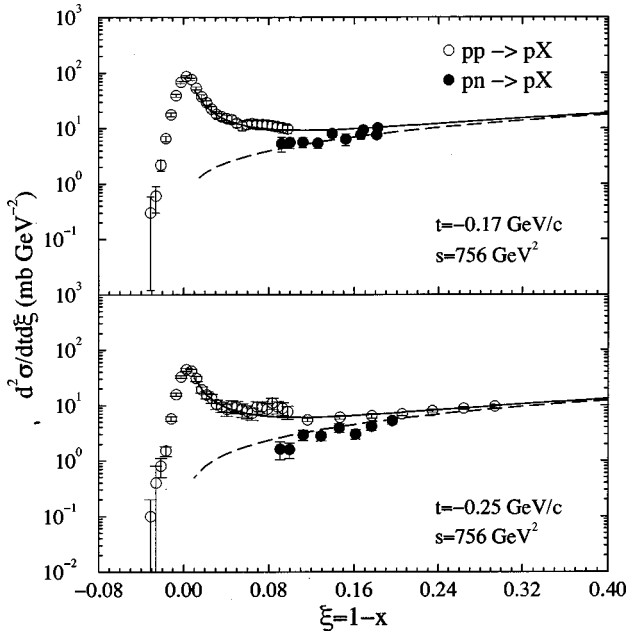

FIG. 1. Invariant cross section for the inclusive reactions $pp \to pX$ (solid curves) and $pn \to pX$ (dashed curves). The solid curves are obtained from Eqs. (A8), (A14), and (A16) which correspond to the Pomeron, pion, and Reggeon contributions, respectively. The dashed curves require only the pion and the Reggeon contributions. These plots intend to put in evidence the differences between these reactions that occur at the diffractive region.

$$E\frac{d^3\sigma}{d\mathbf{p}^3}=\sum_{i,j}\ \gamma_{ij}(m_T^2)\left|\frac{t}{s_0}\right|^{\alpha_i(0)-1}\left|\frac{u}{s_0}\right|^{\alpha_j(0)-1}, \qquad (1)$$

where $m_T=(p_T^2+m_p^2)^{1/2}$ is the transversal mass, and $t=-m_T\sqrt{s}e^{y}$ and $u=-m_T\sqrt{s}e^{-y}$ are the Mandelstam variables given in terms of the rapidity $y=\ln(E+p_L)/m_T$. The contributions considered in our analysis [1] correspond to $i,j=\mathbb{P},\mathbb{R}$, that is double Pomeron, double Reggeon and crossed terms.

For the fragmentation region, we have applied the triple Reggeon model whose cross section has the following general expression:

$$\left(\frac{d^2\sigma}{dtdM^2/s}\right)_{kk\mathbb{P}}=f_k(M^2/s,t)\sigma_{kp}(M^2), \qquad (2)$$

in which $f_k(M^2/s,t)$ is the so-called flux factor, given by

$$f_k(M^2/s,t)=\frac{\beta_k^2}{16\pi}F^2(t)\left(\frac{M^2}{s}\right)^{1-2\alpha_k(t)}, \qquad (3)$$

where β_k is the coupling constant and $F(t)$ is the form factor. These quantities are specific of each contribution and are determined according to $k=\mathbb{P},\mathbb{R},\pi$.

A particular attention was paid to the diffractive region which is dominated by the triple Pomeron contribution ($k=\mathbb{P}$). In this case, we followed the renormalization scheme proposed in Ref. [6] due to the specific problems to describe the experimental data in such a region. For details and particularities about this and the other contributions we refer the reader to the Appendix A and Ref. [1].

In Figs. 1 and 2, we show how the theoretical approach outlined above compares to some of the experimental data [7,8]. In Fig. 1, we point out (for two different t-values) the diffractive behavior in the reaction $pp \to pX$, which is absent from the reaction $pn \to pX$. This difference is important for the calculation that will be described in the next section. Figure 2 shows how the different contributions combine to compose the flat spectrum exhibited by the cross section $d\sigma/dx$ for the reaction $pp \to pX$.

III. BC MODEL APPLIED TO THE FGS APPROACH

As mentioned in the Introduction, in order to describe the invariant cross section for the inclusive reaction proton-nucleus, $pA \to pX$, we make use of an approach developed in Refs. [2–4] that takes into account the multiple scattering effects supposed to happen inside the nucleus. The FGS version of this approach [4] (which is used here) consists basically of a generalization of the Hüfner-Klar model [3] to $pA \to NX$, where N stands for either proton or neutron.

In this kind of process, the scattered nucleon (N) is specified by its transversal momentum, p_T, and by the fraction of the longitudinal momentum, x. In a similar way to what is done in Ref. [4], we express the invariant cross section of such a process as

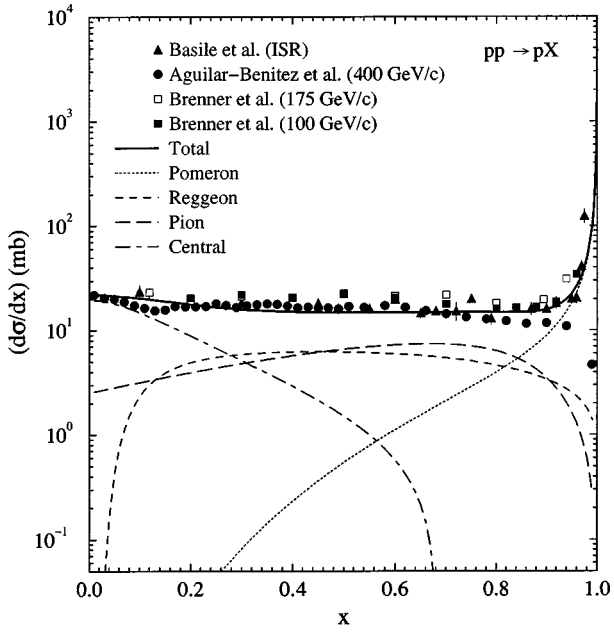

FIG. 2. Leading proton spectrum obtained from the reaction $pp \to pX$. The broken curves, calculated for $\sqrt{s}=15$ GeV, correspond to the central, Pomeron, pion, and Reggeon, contributions which are obtained from Eqs. (A7), (A8), (A14), and (A16), respectively. The continuous curve is the result obtained by adding all contributions up. Data are taken from references quoted in [8].

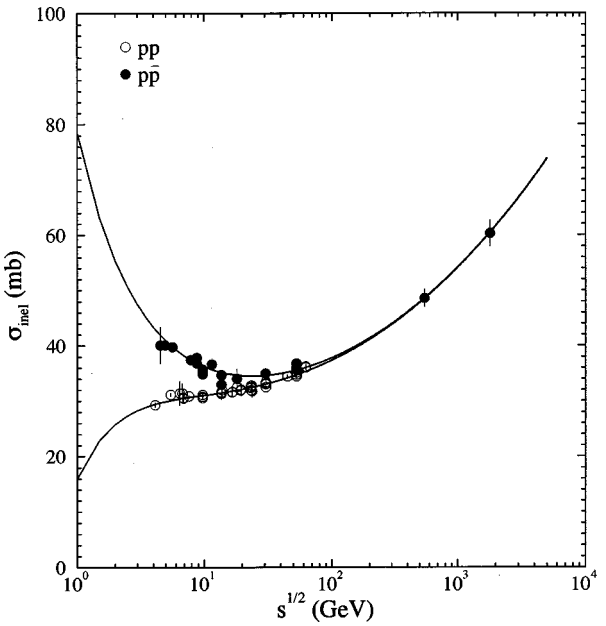

FIG. 3. Inelastic cross section for pp and $p\bar{p}$ scattering. The curves correspond to the parametrizations given by Eq. (7) and the data are from [10].

$$\frac{d^3\sigma}{dxdp_T^2}(pA\to NX)=\sum_{\nu=1}^{A}\sigma_\nu^{pA}D_\nu^N(x,p_T^2). \tag{4}$$

The modifications that we are going to introduce in the FGS model resides specifically in the distribution $D_\nu^N(x,p_T^2)$. The partial cross section, σ_ν^{pA}, is calculated as in Ref. [9] with minor differences in the nuclear densities (see Appendix B). The expression is

$$\sigma_\nu^{pA}=\int d^2b\frac{A!}{\nu!(A-\nu)!}P_A^\nu(1-P_A)^{A-\nu}, \tag{5}$$

in which

$$P_A(b)=\sigma_{pp}^{\rm inel}\int_{-\infty}^{\infty}dz\rho_A(z,b). \tag{6}$$

In Eq. (6) and wherever the cross section $\sigma_{pp}^{\rm inel}$ appears in the following, we use our own parametrization:

$$\sigma_{p\pm p}^{\rm inel}=12.37\,s^{0.104}+34.90\,s^{-0.20}\mp 31.30\,s^{-0.54}\ \ ({\rm mb}), \tag{7}$$

which is compared with data [10] in Fig. 3. This parametrization is proposed here to be consistent with the Pomeron intercept $\epsilon=0.104$ taken from [11] and used to describe the Pomeron contribution in the BC model.

Now we come to the main part of our argument to establish how the cross section given by Eq. (4) is calculated. First we assume that for $\nu=1$, the distributions $D_1^N(x,p_T^2)$ ($N=p,n$) are established from the normalized cross section

$$D_1^N(x,p_T^2)=\frac{1}{\sigma_{\rm inel}^{pp}}\left(\frac{d^3\sigma}{dxdp_T^2}\right)^{pN\to pX}, \tag{8}$$

which in turn were previously fixed from data of the reactions $pp\to pX$ e $pn\to pX$ as shown in Sec. II and in Ref. [1]. As for $\nu>1$, we assume that the recurrence formulas from FGS approach apply, that is

$$D_\nu^p(x,p_T^2)=\int_x^1\frac{dy}{y}[n_1^pS_{\nu-1}^+(y)D_{\nu-1}^p(x/y,p_T^2)+n_1^nS_{\nu-1}^-(y)D_{\nu-1}^n(x/y,p_T^2)] \tag{9}$$

and

$$D_\nu^n(x,p_T^2)=\int_x^1\frac{dy}{y}[n_1^pS_{\nu-1}^+(y)D_{\nu-1}^n(x/y,p_T^2)+n_1^nS_{\nu-1}^-(y)D_{\nu-1}^p(x/y,p_T^2)]. \tag{10}$$

In the expressions above, the functions $S_\nu^{+,-}(y)$ are defined as

$$S_\nu^{+,-}(y)=\frac{y^{\alpha_\nu}M_1^{p,n}(y)}{\int_0^1dyy^{\alpha_\nu}M_1^{p,n}(y)}, \tag{11}$$

with $\alpha_0=0$ and $\alpha_\nu(\nu\geqslant 1)$ as the (unique) free parameter. The distribution $M_1^{p,n}(y)$ comes from

$$M_\nu^{p,n}(y)=\int D_\nu^{p,n}(y,p_T^2)dp_T^2, \tag{12}$$

and the parameters n_1^p and n_1^n that appear in Eqs. (9) and (10) pondering the contributions are the multiplicities given by

$$n_\nu^{p,n}=\int_0^1M_\nu^{p,n}(x)dx. \tag{13}$$

By integrating Eqs. (9) and (10) over p_T, one obtains the recurrence relations for the longitudinal distributions as originally proposed in the FGS model, that is

$$M_\nu^p(x)=\int_x^1\frac{dy}{y}[n_1^pS_{\nu-1}^+(y)M_{\nu-1}^p(x/y)+n_1^nS_{\nu-1}^-(y)M_{\nu-1}^n(x/y)] \tag{14}$$

and

$$M_\nu^n(x)=\int_x^1\frac{dy}{y}[n_1^pS_{\nu-1}^+(y)M_{\nu-1}^n(x/y)+n_1^nS_{\nu-1}^-(y)M_{\nu-1}^p(x/y)], \tag{15}$$

from which one may calculate the cross section

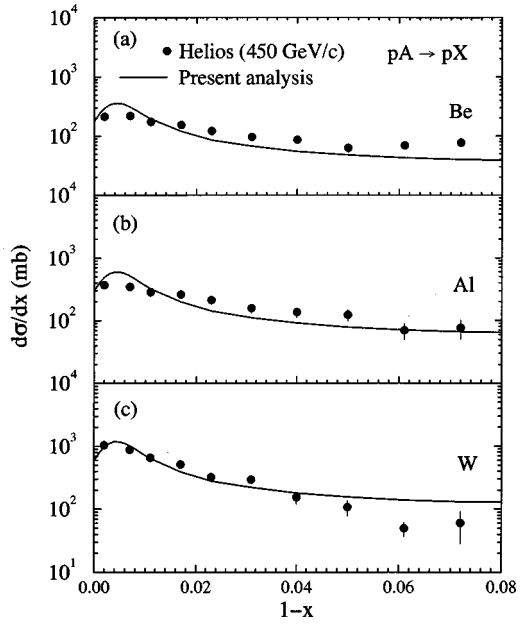

FIG. 4. Differential cross section for diffractive dissociation of nuclei obtained with the FGS/BC approach in comparison to experimental data from the HELIOS Collaboration [12].

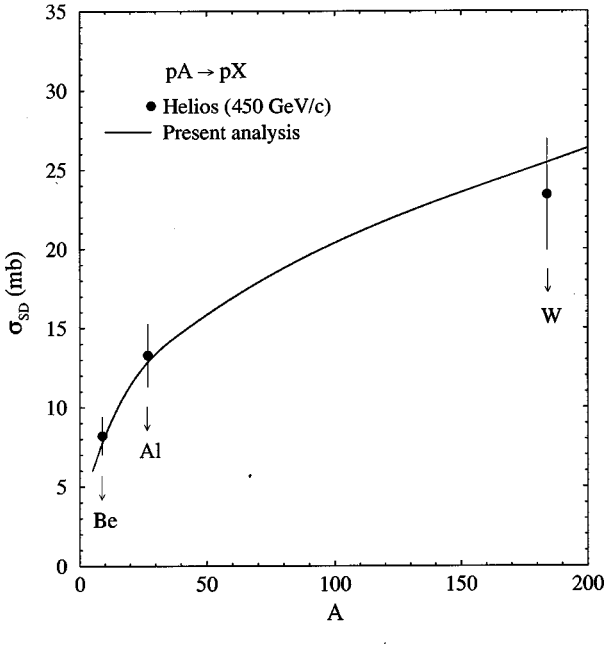

FIG. 5. Integrated diffractive cross section vs atomic mass *A*. The curve is obtained by the integration of the differential cross section $d\sigma/dx$ within the experimental limits. The data are from HELIOS Collaboration [12].

$$\frac{d\sigma}{dx}(pA\to NX)=\sum_{\nu=1}^{A}\sigma_{\nu}^{pA}M_{\nu}^{N}(x). \tag{16}$$

Although we have introduced modifications in the FGS model by defining the distributions already at the level of $\nu=1$, that is $D_1^N(x,p_T^2)$ or equivalently $M_1^N(x)$, one may consistently specify the boundary conditions as

$$M_0^p(x)=\delta(1-x) \quad \text{and} \quad M_0^n(x)=0. \tag{17}$$

One can easily see that the approach given by Eqs. (14)–(17), namely the FGS model, corresponds to a generalization of the Hüfner-Klar model [3] that suitably includes the preservation or changing in the leading particle isospin. This generalization was proposed in terms of the longitudinal distributions $M_\nu^N(x)$. With our modifications, proposed in the Eqs. (4)–(13), we intend to show that the validity of such a theoretical scheme can be extended to distributions dependent on both variables, that is to $D_\nu^N(x,p_T^2)$. This is shown in the next section.

IV. RESULTS AND DISCUSSION

A. Cross sections

We start this section by presenting the results for diffractive dissociation in nuclear processes obtained with the approach outlined above. As we shall see, a good description of the data in the fragmentation region requires a (at least) reasonable description for the diffractive spectrum. In Fig. 4, it is shown the diffractive cross section predictions for Beryllium, Aluminum, and Tungsten in comparison to the experimental data obtained by the HELIOS Collaboration [12]. In Fig. 5, the integrated cross section is compared to data of the same experiment, showing a perfect agreement.

Some clarifications about these calculations are in order. First of all we emphasize that no free parameter was used to obtain such a description. It was obtained basically by introducing the leading proton spectrum (as it is given by the BC model) into the FGS formalism and by taking $\nu=1$. This last assumption ($\nu=1$) is also used in the FGS analysis [4] and is justified by the fact that the diffractive dissociation of a nucleus seems to occur as a result of the excitation of single nucleons on its rim (see [12] and [13]).

Another important point here is that the renormalized flux factor, as it is described in Refs. [6,14], was applied to the diffractive cross section as well as the convolution procedure that takes into account the resolution effects in the determination of the (recoiling) proton momentum in the region of $x\approx 1$ (see [14]).

Although the agreement with data shown in Fig. 4 is not perfect, it is good enough to propitiate an excellent description of the data in the fragmentation region, which is presented in the following.

The description of the cross section in the fragmentation region requires full implementation of the FGS formalism. We show the theoretical predictions compared to data of two different experiments: in Fig. 6, the longitudinal spectrum is compared to data of Ref. [15] and, in Fig. 7, the invariant cross section is compared to data of Ref. [16] for two different p_T values. As we see, particularly in Fig. 6 the agreement with the data is pratically perfect, while in Fig. 7 it is quite reasonable too. In order to obtain such results we have performed the sum in Eq. (4) up to $\nu=8$ since the contributions beyond this value are negligible. In Fig. 8, it is shown

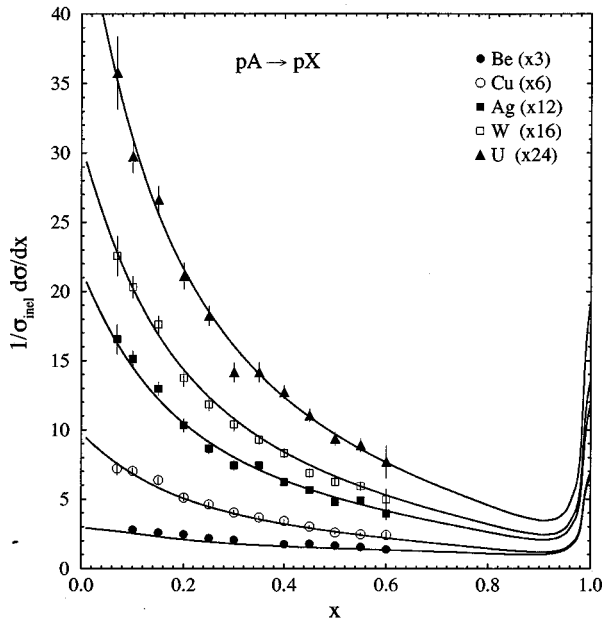

FIG. 6. Leading proton spectrum for the reactions $pA \rightarrow pX$ ($A = \mathrm{Be, Cu, Ag, W, U}$). The curves are determined from the FGS/BC approach (as described in the text) for $\sqrt{s} = 15$ GeV and the experimental data are from Ref. [15]. The data were shifted as shown in the figure for clarity.

the x-dependence of these contributions and the final result for the uranium case.

The results shown above were obtained by fixing the free parameter that appears in Eq. (11) as $\alpha_\nu = 2.6$ ($\nu \geqslant 1$) for the data of Fig. 6. This is a remarkable outcome if we consider

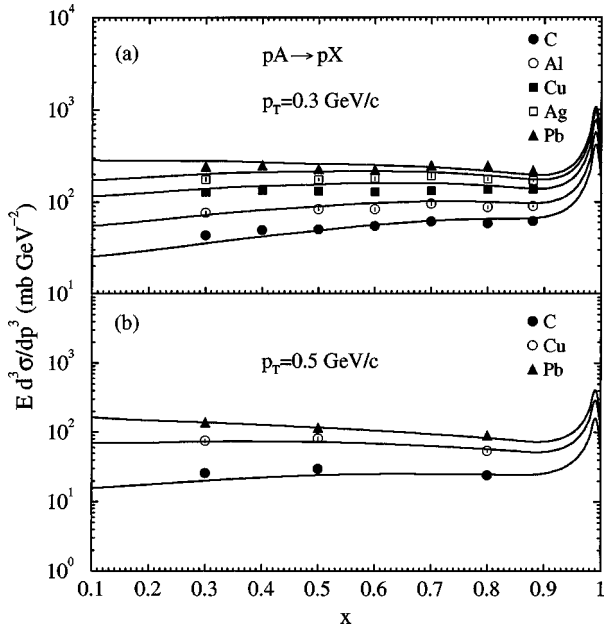

FIG. 7. Invariant cross section for the inclusive reactions $pA \rightarrow pX$ ($A = \mathrm{C, Al, Cu, Ag, Pb}$) as given by the FGS/BC approach in comparison to data experimental [16] for two p_T values. Data and theoretical calculation correspond to $\sqrt{s} = 14$ GeV.

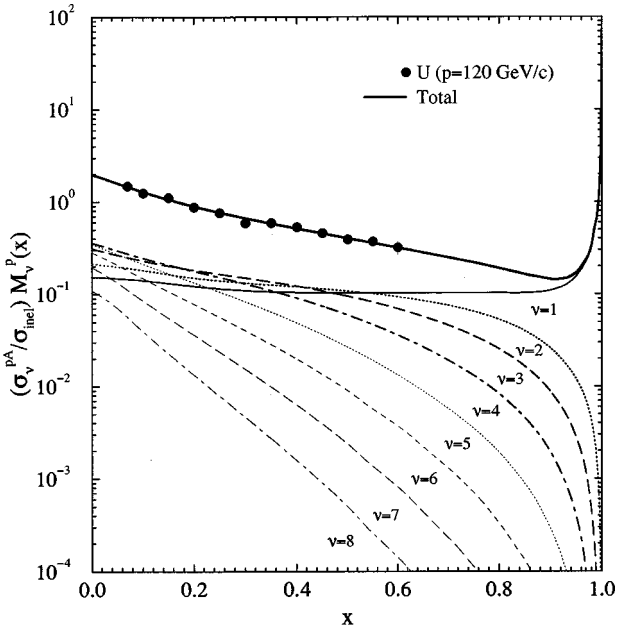

FIG. 8. Leading proton spectrum obtained from the reaction $pU \rightarrow pX$. It is shown the behavior of the contributions calculated from $\nu = 1$ to $\nu = 8$ as they appear in Eq. (4). Data are from [15].

that, to pass from a description of the inclusive reaction $pp \rightarrow pX$ (obtained in a totally independent way) to the description of nuclear reactions of the type $pA \rightarrow pX$, only one free parameter was necessary. After fixing α_ν, the curves presented in Fig. 7 were calculated directly, without any other adjustment. This tells us that Eqs. (9) and (10) works pretty well and, therefore, that the same scheme of calculations that is used to obtain $M_\nu^{p,n}(x)$ can be successfully applied to $D_\nu^{p,n}(x, p_T^2)$ as well.

In short, all of this shows how good the FGS approach is in taking into account the multiple scattering effects.

Back to the parameter α_ν, we note (like in [4]) that its role is making harder the spectrum inside the nucleus. Since it is indispensable to describe the data, we conclude that the elasticities of the intranuclear collisions are not the same as for free particles. We discuss this point in more detail below.

Another point to be mentioned about these calculations is that, for the energy at which the data of Fig. 6 were taken, the corresponding leading particle multiplicities are $n_1^p = 0.56$ and $n_1^n = 0.44$, and that makes exactly $n_1^p + n_1^n = 1$. However, this result is accidental since these multiplicities were calculated independently and directly from the BC model; and furthermore they change with energy.[3] Differently from what was done in the FGS analysis [4], in our calculations we did not impose any constraints on the multiplicities so that they were left free to change with the energy as determined by the BC model.

[3]The energy evolution of n_1^p can be seen in Fig. 8 of Ref. [1]. Notice, however, that the values given there correspond to two hemispheres and therefore should be divided by 2.

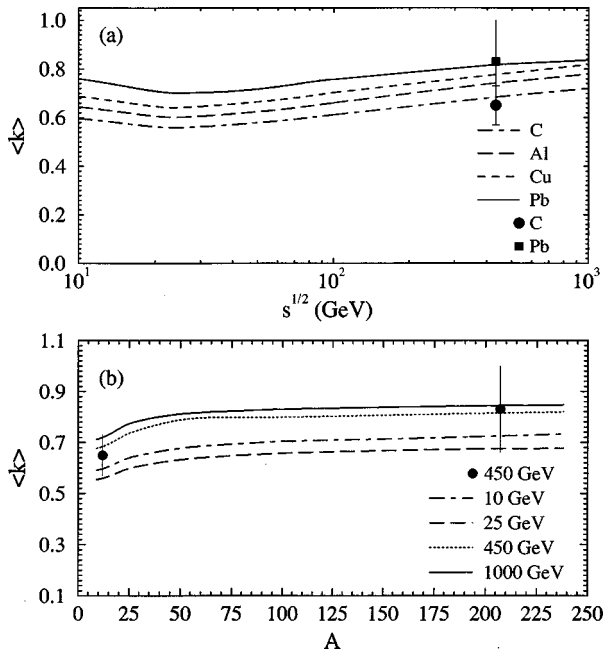

FIG. 9. Behavior of the average inelasticity in terms of (a) energy, $\sqrt{s}$, and (b) atomic mass, A. The experimental data, from [17,18], refer to carbon and lead nuclei and were measured at $\sqrt{s}\sim 450$ GeV.

B. Average inelasticity

Average inelasticity, a quantity that is employed in the calculation of cascades developed in the atmosphere, is usually defined as the fraction of energy used for multiparticle production in every collision. Due to the lack of experimental data, it is difficult to establish how this quantity is obtained and how it should evolve with energy. This difficulty is noticeable by the enduring debate going on in the literature (see, for instance, the papers about this subject quoted in [1]).

In the present analysis, we define the total average inelasticity as

$$\langle k\rangle = 1-\langle x\rangle = 1-\frac{1}{\sigma_{\rm incl}}\int x\frac{d\sigma^{\,pA\to pX}}{dx}\,dx, \tag{18}$$

where the inclusive cross sections $(d\sigma/dx)^{pA\to pX}$ correspond to those curves presented in Fig. 6, but normalized by the integrated inclusive cross section $\sigma_{\rm incl}\equiv\int(d\sigma/dx)dx$.

The way the average inelasticity evolves with the energy $\sqrt{s}$ and with atomic mass A is shown in Fig. 9. In both cases a mild increasing of $\langle k\rangle$ is observed. Two experimental points [17,18] are given for comparison, $\langle k_C\rangle = 0.65\pm 0.08$ from [17] and $\langle k_{Pb}\rangle = 0.83\pm 0.17$ from [18].

C. Partial inelasticity

The concept of partial inelasticity was firstly defined in the Hüfner-Klar model [3] by the relation

$$\langle x\rangle_\nu = (1-I)\langle x\rangle_{\nu-1}. \tag{19}$$

Actually, in Ref. [3], I is one of the free parameters that is adjusted to describe the data and physically represents a measure of the nuclear stopping power since it gives the rate of energy loss after every intranuclear collision.

In the FGS model, an analogous quantity based on the interplay of Eqs. (14) and (15) is also defined. However, there is a bit of confusion in such a definition which we try to clarify below. After introducing the mean value

$$\langle x\rangle_\nu^{p,n} = \int_0^1 dx x M_\nu^{p,n}(x), \tag{20}$$

the authors present the relation (see [4])

$$[n_\nu^p\langle x\rangle_\nu^p + n_\nu^n\langle x\rangle_\nu^n] = (1-I_\nu)[n_{\nu-1}^p\langle x\rangle_{\nu-1}^p + n_{\nu-1}^n\langle x\rangle_{\nu-1}^n], \tag{21}$$

in which I_ν is said to be given by

$$I_\nu = 1-\mathbf{S}_p^+ - \mathbf{S}_n^- \tag{22}$$

with

$$\mathbf{S}_p^+ = n_1^p\int_0^1 dy y S_{\nu-1}^+(y), \quad \text{and} \quad \mathbf{S}_n^- = n_1^n\int_0^1 dy y S_{\nu-1}^-(y). \tag{23}$$

The reader will easily identify Eqs. (21)–(23) above with Eqs. (20) and (21) of Ref. [4].

The problematic point here is that the expressions for I_ν that comes from Eqs. (21) and (22) are inconsistent with each other. Perhaps the easiest way to verify such a statement is by putting $\nu=1$ in both expressions and comparing the results. Since no details about these calculations appear in [4], we give below our own interpretation about a possible origin for such a problem.

First we note that by applying the definition of the mean value $\langle x\rangle$ given by Eq. (20) to the Eqs. (14) and (15), it is possible to manipulate the outcomes to work out the relation

$$\langle x\rangle_\nu^p + \langle x\rangle_\nu^n = [\mathbf{S}_p^+ + \mathbf{S}_n^-]^\nu. \tag{24}$$

This relation is crucial to what follows.

From the above equation, we define a kind of *average nucleonic inelasticity* K_ν given by[4]

$$(1-K_\nu) \equiv \frac{\langle x\rangle_\nu^p + \langle x\rangle_\nu^n}{\langle x\rangle_{\nu-1}^p + \langle x\rangle_{\nu-1}^n} = \mathbf{S}_p^+ + \mathbf{S}_n^-. \tag{25}$$

It is immediately seen that K_ν so defined corresponds exactly to I_ν given by Eq. (22). Now let us introduce the *normalized* mean value

[4]Such a definition should not be confused with $\langle k\rangle$ given by Eq. (18). The latter is a quantity that refers to the inclusive process $pA\to pX$ as a whole, whereas K_ν has to do with putative intranuclear collisions.

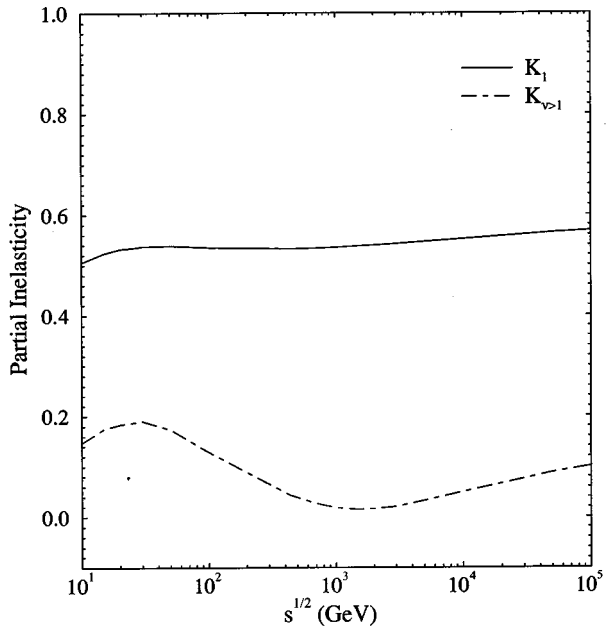

FIG. 10. Behavior of the partial inelasticities K_1 and $K_{\nu>1}$ in terms of energy.

$$\langle \tilde{x} \rangle_\nu^{p,n} \equiv \frac{\int_0^1 dx x M_\nu^{p,n}(x)}{\int_0^1 dx M_\nu^{p,n}(x)} = \frac{\langle x \rangle_\nu^{p,n}}{n_\nu^{p,n}}, \tag{26}$$

which implies

$$\langle x \rangle_\nu^{p,n} = n_\nu^{p,n} \langle \tilde{x} \rangle_\nu^{p,n}. \tag{27}$$

By replacing Eq. (27) in Eq. (25), one gets the relation

$$[n_\nu^p \langle \tilde{x} \rangle_\nu^p + n_\nu^n \langle \tilde{x} \rangle_\nu^n] = (1 - K_\nu)[n_{\nu-1}^p \langle \tilde{x} \rangle_{\nu-1}^p + n_{\nu-1}^n \langle \tilde{x} \rangle_{\nu-1}^n], \tag{28}$$

which is basically the same as Eq. (21), with exception of the definition of the mean value of x. Thus, it seems clear from the reasoning presented above that the mentioned inconsistency in the definitions of I_ν comes from an ambiguity (probably involuntary) in the treatment of $\langle x \rangle$. Be that as it may, we apply in our calculations the definition (25), which corresponds to the FGS expression (22).

In Fig. 10, we show the results obtained for K_1 and $K_{\nu>1}$ obtained from Eq. (25). Roughly speaking, the main result is that K_1 is on average five times larger than $K_{\nu>1}$. K_1 exhibits a pretty mild behavior while $K_{\nu>1}$ in turn presents a fall off with energy up to $\sqrt{s} \sim 10^3$ GeV, which is similar to the results shown in the FGS analysis [4]. Beyond this energy, FGS results continue to fall while our calculations indicate a sensible increasing with energy.

Finally, we note that both theoretical results are rather small in comparison to a recent experimental estimation which gives $K_{\nu>1} \simeq 0.2$ at $\sqrt{s} \sim 450$ GeV [17]. However, it should also be noted that they agree with this experiment in a more general sense since it is clearly established that $K_{\nu>1}$ is much less than K_1.

V. SUMMARY

In this paper, we have presented an extension of a previous analysis [1] on the inclusive reaction $pp \to pX$ (here called the BC model) to nuclear processes of the type $pA \to pX$. In order to do that, we have used an approach to take into account the multiple scattering effects inside the nuclear matter that was proposed initially by Hwa [2] and developed by Hüfner and Klar [3], and Frichter, Gaisser, and Stanev (FGS model) [4].

By using the last version of such an approach, we have shown that a combination of the BC and FGS models makes up a theoretical framework that requires only one free parameter to provide a quite precise description of the inclusive nuclear processes analized. Besides the agreement with cross section data, the consistency obtained with experimental results of average inelasticity, $\langle k \rangle$, and partial inelasticities, K_ν, indicates that the combined FGS/BC model constitutes a theoretical framework quite appropriate to compute the multiple scattering effects of intranuclear collisions.

ACKNOWLEDGMENTS

We would like to thank the Brazilian governmental agencies CNPq and FAPESP for financial support.

APPENDIX A: CROSS SECTIONS

In this appendix we present the main expressions used to calculated the cross section for the inclusive process $pp \to pX$ as they were applied in our previous paper [1].

1. Central region

For the central region, we use the invariant cross section given by the double Reggeon model [5], that is

$$E \frac{d^3\sigma}{d\mathbf{p}^3} = \sum_{i,j} \gamma_{ij}(m_T^2) \left| \frac{t}{s_0} \right|^{\alpha_i(0)-1} \left| \frac{u}{s_0} \right|^{\alpha_j(0)-1}, \tag{A1}$$

in which the coupling function $\gamma_{ij}(m_T^2)$ assumes a Gaussian form,

$$\gamma_{ij}(m_T^2) = \Gamma_{ij} e^{-a_{ij} m_T^2}. \tag{A2}$$

From Eq. (A1), the invariant cross sections for the contributions obtained with $i,j = \mathbb{P}, \mathbb{R}$ become

$$\left(E \frac{d^3\sigma}{d\mathbf{p}^3} \right)_{\mathbb{PP}} = \Gamma_{\mathbb{PP}} e^{-a_{\mathbb{PP}} m_T^2} (m_T \sqrt{s})^{2\epsilon}, \tag{A3}$$

$$\left(E \frac{d^3\sigma}{d\mathbf{p}^3} \right)_{\mathbb{PR}+\mathbb{RP}} = 2\Gamma_{\mathbb{PR}} e^{-a_{\mathbb{PR}} m_T^2} (m_T \sqrt{s})^{\epsilon + \alpha_{\mathbb{R}}(0) - 1} \times \cosh[(1 + \epsilon - \alpha_{\mathbb{R}}(0) y)], \tag{A4}$$

TABLE I. Values of the parameters Γ_{ij} and a_{ij}.

ij	Γ_{ij} (mb GeV^{-2})	a_{ij} (GeV^{-2})
$\mathbb{PP}$	23.53	3.90
$\mathbb{PR}$	−29.8	3.45
$\mathbb{RR}$	13.75	1.80

and

$$\left(E\frac{d^3\sigma}{d\mathbf{p}^3}\right)_{\mathbb{RR}} = \Gamma_{\mathbb{RR}} e^{-a_{\mathbb{RR}} m_T^2} (m_T\sqrt{s})^{2(\alpha_{\mathbb{R}}(0)-1)}. \quad \text{(A5)}$$

In the above expressions $\alpha_{\mathbb{IR}}(0)=0.5$ and $\epsilon=0.104$ [11]. The other constants are adjusted to describe the data of the reaction $pp\to\overline{p}X$ (whose production mechanism is typically central) through the expression

$$\left(E\frac{d^3\sigma}{d\mathbf{p}^3}\right)^{\text{central}}_{pp->\overline{p}X} = \left(E\frac{d^3\sigma}{d\mathbf{p}^3}\right)_{\mathbb{PP}} + \left(E\frac{d^3\sigma}{d\mathbf{p}^3}\right)_{\mathbb{PR}+\mathbb{RP}} + \left(E\frac{d^3\sigma}{d\mathbf{p}^3}\right)_{\mathbb{RR}}. \quad \text{(A6)}$$

These constants are given in Table I.

Then, in order to obtain the central part of the cross section for the process $pp\to pX$, we make

$$\left(E\frac{d^3\sigma}{d\mathbf{p}^3}\right)^{\text{central}}_{pp->pX} = \lambda(s)\left(E\frac{d^3\sigma}{d\mathbf{p}^3}\right)^{\text{central}}_{pp->\overline{p}X}, \quad \text{(A7)}$$

in which $\lambda(s)$ is parametrized as $\lambda(s)=1.0+11.0s^{-0.3}$.

2. Fragmentation region

The invariant cross section for the fragmentation region is compounded of three predominant contributions which are determined within the triple Reggeon model [5]. These contributions correspond to Pomeron, pion and Reggeon exchanges and are referred to as $\mathbb{PPP}$, $\pi\pi\mathbb{P}$, $\mathbb{RRP}$, respectively.

The $\mathbb{PPP}$ contribution, which is dominant in the diffractive region, is given by

$$\left(\frac{d^2\sigma}{dtd\xi}\right)_{\mathbb{PPP}} = f_{\mathbb{P},\text{ren}}(\xi,t)\times\sigma_{\mathbb{P}p}(s\xi), \quad \text{(A8)}$$

where $f_{\mathbb{P},\text{ren}}(\xi,t)$ is the *renormalized* Pomeron flux factor proposed in [6] with the parameters defined in [19], that is

$$f_{\mathbb{P},\text{ren}}(\xi,t) = \frac{f_{\mathbb{P}}(\xi,t)}{N(s)} \quad \text{(A9)}$$

with the Donnachie-Landshoff flux factor [20]

$$f_{\mathbb{P}}(\xi,t) = \frac{\beta_0^2}{16\pi}F_1^2(t)\xi^{1-2\alpha_{\mathbb{P}}(t)} \quad \text{(A10)}$$

and

$$N(s) = \int_{1.5/s}^{1}\int_{-\infty}^{t=0} f_{\mathbb{P}}(\xi,t)dtd\xi. \quad \text{(A11)}$$

In the above expressions, $F_1(t)$ is the Dirac form factor,

$$F_1(t) = \frac{(4m^2-2.79t)}{(4m^2-t)}\frac{1}{\left(1-\frac{t}{0.71}\right)^2}, \quad \text{(A12)}$$

the Pomeron trajectory is $\alpha_{\mathbb{P}}(t)=1+\epsilon+\alpha' t$ with $\epsilon=0.104$, $\alpha'=0.25$ GeV^{-2}, and $\beta_0=6.56$ GeV^{-1}, determined from [19]. In Eq. (A8), the Pomeron-proton cross section is given by

$$\sigma_{\mathbb{P}p}(M^2) = \beta_0 g_{\mathbb{P}}(s\xi)^{\epsilon} \quad \text{(A13)}$$

with the triple Pomeron coupling determined from data as $g_{\mathbb{P}}=0.9$ GeV^{-1}.

The pion contribution ($\pi\pi\mathbb{P}$) is given by [21]

$$\left(\frac{d^2\sigma}{dtd\xi}\right)_{\pi\pi\mathbb{P}} = f_{\pi}(\xi,t)\times\sigma_{\pi p}(s\xi), \quad \text{(A14)}$$

where

$$f_{\pi}(\xi,t) = \frac{1}{4\pi}\frac{g^2}{4\pi}\frac{|t|}{(t-\rho^2)^2}e^{b_{\pi}(t-\rho^2)}\xi^{1-2\alpha_{\pi}(t)} \quad \text{(A15)}$$

and $\alpha_{\pi}(t)=0.9(t-\rho^2)$ with $\rho^2=m_{\pi}^2=0.02$ GeV^2. We follow [21] putting $g^2/4\pi=15.0$ and $b_{\pi}=0$. The pion-proton cross section $\sigma_{\pi p}(s\xi)=10.83(s\xi)^{0.104}+27.13(s\xi)^{-0.32}$ (mb) is taken from [11].

The Reggeon contribution ($\mathbb{RRP}$) is determined by

$$\left(\frac{d^2\sigma}{dtd\xi}\right)_{\mathbb{RRP}} = f_{\mathbb{R}}(\xi,t)\times\sigma_{\mathbb{R}p}(s\xi), \quad \text{(A16)}$$

with

$$f_{\mathbb{R}}(\xi,t) = \frac{\beta_{0\mathbb{R}}^2}{16\pi}e^{2b_{\mathbb{R}}t}\xi^{1-2\alpha_{\mathbb{R}}(t)} \quad \text{(A17)}$$

and

$$\sigma_{\mathbb{R}p}(s\xi) = \beta_{0\mathbb{R}}g_{\mathbb{R}}(s\xi)^{\epsilon}. \quad \text{(A18)}$$

In this case, the trajectory is assumed to be $\alpha_{\mathbb{R}}(t)=0.5+t$ while the constants $\beta_{\mathbb{R}}\equiv(\beta_{0\mathbb{R}}^3 g_{\mathbb{R}})$ and $b_{\mathbb{R}}$ (determined from data) are $\beta_{\mathbb{R}}=2465.7$ mb GeV^{-2} and $b_{\mathbb{R}}=0.1$ GeV^{-2}.

APPENDIX B: NUCLEAR DENSITIES

The nuclear densities applied in our calculation are similar to those used in [9]. In Eq. (6), the nuclear density used

for light nuclei ($6 \leqslant A \leqslant 18$) is

$$\rho(r) = \frac{4}{\pi^{3/2} a_0^3} \left[1 + \frac{1}{6}(A-4) \frac{r^2}{a_0^2} \right] \exp(-r^2/a_0^2), \quad \text{(B1)}$$

with $a_0 = [(r_0^2 - r_p^2)^{1/2}/(5/2 - 4/A)]^{1/2}$, $r_0 = 1.2A^{1/3}$ fm, and $r_p = 0.8$ fm.

For heavier nuclei ($A \geqslant 18$), $\rho(r)$ is calculated according to the Woods-Saxon formula [22], that is

$$\rho(r) = \frac{c_0}{1 + \exp[(r - r_0)/b_0]}, \quad \text{(B2)}$$

where c_0 is the normalization constant

$$c_0 = \frac{3}{4\pi r_0^3} \frac{1}{1 + (b_0 \pi / r_0)^2} \quad \text{(B3)}$$

and $b_0 = 0.4$ fm.

[1] M. Batista and R. J. M. Covolan, Phys. Rev. D **59**, 054006 (1999).

[2] R. C. Hwa, Phys. Rev. Lett. **52**, 492 (1984).

[3] J. Hüfner and A. Klar, Phys. Lett. **145B**, 167 (1984).

[4] G. M. Frichter, T. K. Gaisser, and T. Stanev, Phys. Rev. D **56**, 3135 (1997).

[5] P. D. B. Collins, *An Introduction to Regge Theory and High Energy Physics* (Cambridge University Press, Cambridge, England, 1977); P. D. B. Collins and A. D. Martin, *Hadron Interactions* (Adam Hilger Ltd., Bristol, England, 1984).

[6] K. Goulianos, Phys. Lett. B **358**, 379 (1995).

[7] B. Robinson *et al.*, Phys. Rev. Lett. **34**, 1475 (1975); J. C. M. Armitage *et al.*, Nucl. Phys. **B194**, 365 (1982).

[8] M. Basile *et al.*, Phys. Lett. **95B**, 31 (1980); Nuovo Cimento A **65**, 500 (1981); M. Aguilar-Benitez *et al.*, Z. Phys. C **50**, 405 (1991); A. E. Brenner *et al.*, Phys. Rev. D **26**, 1497 (1982).

[9] J. Engel *et al.*, Phys. Rev. D **46**, 5013 (1992).

[10] Particle Data Group, C. Caso *et al.*, Eur. Phys. J. C **3**, 207 (1998); data available electronically from http://pdg.lbl.gov/xsect/contents.html

[11] R. J. M. Covolan, J. Montanha, and K. Goulianos, Phys. Lett. B **389**, 176 (1996).

[12] HELIOS Collaboration, T. Akesson *et al.*, Z. Phys. C **49**, 355 (1991).

[13] R. J. M. Covolan and J. Montanha, Phys. Rev. D **53**, 6127 (1996).

[14] K. Goulianos and J. Montanha, ''Factorization and Scaling in Hadronic Diffraction,'' Rockefeller University Report No. RU 97/E-43, hep-ph/9805496, Phys. Rev. D (to be published).

[15] R. Bailey *et al.*, Z. Phys. C **29**, 1 (1985).

[16] D. S. Barton *et al.*, Phys. Rev. D **27**, 2580 (1983).

[17] G. Wilk and Z. Włodarczyk, Phys. Rev. D **59**, 014025 (1999).

[18] Chacaltaya Cosmic Ray Collaboration, S. L. C. Barroso *et al.*, in Proceedings of the 25th International Cosmic Ray Conference, Durban, 1997, edited by M. S. Potgieter, B. C. Raubenheimer, and D. J. van der Walt, Vol. 6 (HE Sessions), p. 41.

[19] R. J. M. Covolan and M. S. Soares, Phys. Rev. D **57**, 180 (1998).

[20] A. Donnachie and P. V. Landshoff, Nucl. Phys. **B303**, 634 (1988).

[21] R. D. Field and G. C. Fox, Nucl. Phys. **B80**, 367 (1974).

[22] R. C. Barret and D. F. Jackson, *Nuclear Sizes and Structure* (Oxford University Press, Oxford, 1977).